https://grupo.us.es/grupotep130/es/

A comparison of closed-form and finite-element solutions for heat transfer in a nearly horizontal, unglazed flat plate PVT water collector: Performance assessment

David Moreno, Manuel Fernández, Paula M. Esquivias

This is an **Accepted Manuscript** of an article published by **Elsevier**:

Solar Energy, Volume 141, 2017, Pages 11-24, ISSN 0038-092X,

https://doi.org/10.1016/j.solener.2016.11.015

A comparison of closed-form and finite-element solutions for heat transfer in a nearly horizontal, unglazed flat plate PVT water collector: Performance assessment

Authors' names and affiliations:

David Moreno [a], Manuel Fernández [a], Paula M. Esquivias [a]

[a] Instituto Universitario de Arquitectura y Ciencias de la Construcción (IUACC), Universidad de Sevilla, Spain

Corresponding Author:

David Moreno, Instituto Universitario de Arquitectura y Ciencias de la Construcción (IUACC), Universidad de Sevilla, Spain

Email: davidmoreno@us.es

Abstract

In order to compare the domestic hot water heating (DHW) and the power supply performances of a south-facing unglazed flat-plate PVT installed on a roof, with an 8° gradient belonging to a solar house located in Madrid (40.24N, 3.41O) with no surrounding obstacles, a finite element heat flux simulation was performed and contrasted with a theoretical mathematical model. In this manner, a correlation between the energy absorbed by water within the pipes in the PVT panel and its inlet temperature, dependant on the tank temperature, is approximated.

In both cases, and for certain operating conditions, results are obtained by simulation and by solving the analytical models. The difference between the two methods is used to estimate the degree of freedom introduced. Once the analytical model has been validated by simulation, it is solved for different inlet water temperatures, giving an estimated correlation between the energy absorbed by the Heat Transfer Fluid (HTF) and the solar contribution to DHW.

The results show how using this kind of solar panel not only improves the overall performance of a PVT panel with regard to a PV cell performance alone, but it also enables photovoltaic and solar thermal energy to be incorporated in the same area. This is especially crucial when the roof area is limited or restricted, even when the outlet water temperature for DHW is not excessively high.

Keywords: Energy efficiency, photovoltaic panel, solar thermal panel, hybrid panel, solar decathlon

1 Introduction

Residential buildings consume a significant amount of energy and the use of renewable energy technologies can provide important contributions towards zero or near-zero energy buildings. Solar-powered houses have been the object of several research papers, projects and even competitions

such as Solar Decathlon from the U.S. Department of Energy (2015), encouraging innovations in solar energy systems and their integration into building design.

According to the Solar Thermal Action Plan for Europe (STAP), over 50% of energy production will be based on solar energy (ESTIF 2007) by 2030.Nowadays, solar energy systems are commonly incorporated into buildings, especially roofs, covering large areas for solar collection. This is mainly for thermal purposes, but there is also photovoltaic energy collection. Tall, dense residential buildings face the problem of having an insufficient roof area to hold enough solar panels in order to cover the energy demand. Compared with conventional collectors, one of the advantages of hybrid photovoltaic-thermal (PVT) collectors is that space is saved by integrating a solar thermal water collector and a photovoltaic module into a single device (Antonanzas et al. 2015) (Buker and Riffat 2015) (Chow 2003).

A photovoltaic/thermal (PVT) collector is a combination of photovoltaic (PV) and solar thermal components that simultaneously produce both electricity and heat. PVT collector performance is based on the principle that not only does a PV cell produce electricity with peak efficiencies in the range of 5–20%, but it also acts as a thermal absorber. Much of the captured solar energy in a non-hybrid PV module raises cell temperatures causing degradation in module efficiency. In order to ensure a high electrical output, this residual heat needs to be removed. The transfer of this thermal energy to an HTF provides useful thermal energy for use in low- and medium-temperature applications while also refrigerating the PV cells. This dual function of the PVT enables a more effective use of solar energy, resulting in a higher overall solar conversion (Buker and Riffat 2015)(Antonanzas et al. 2015)(Kalogirou 2001) (Anderson et al. 2009)(Kim et al. 2014)(Santbergen et al. 2010).

There are several approaches to PVT technology. Among many others, the main classification criteria are by HTF, the relative position of the HTF with respect to PV cells, the coverage of the PV cells, the type of PV cells, the shape of PVT collectors, natural or forced fluid flow, stand-alone or building-integrated features. (Antonanzas et al. 2015) (Kumaret al. 2015) (Kim et al. 2014). Water-based PVT modules possess absorbers or heat exchangers in conjunction with a number of PV cells connected in parallel or in series and attached to a serpentine or series of parallel pipes behind, through which water is forced to flow (Kumaret al. 2015). If the water temperature is kept low, PV cells will be cooled, leading to enhanced electrical conversion efficiencies while the water temperature will rise through absorbing heat from the PV cell layer (Buker and Riffat 2015).

PVT collectors have been the object of several studies. Anderson et al. (2009) theoretically analysed a building with an integrated photovoltaic thermal water system (BiPVT/w) in Australia. Results highlighted that good thermal contact between the PV cells and the absorber will improve both the system's electrical and thermal efficiencies. In addition, increasing the transmittance/absorptance product results in the greatest increase in thermal efficiency of all of the parameters assessed, without greatly reducing the electrical efficiency. Furthermore, the use of unglazed BIPVT systems in conjunction with heat pumps could present interesting possibilities.

Zondag et al. (2003) analysed the yield of a system with flat-plate PVT collectors using water as the HTF for Dutch climatic conditions. The authors concluded that the one-cover glazed sheet-and-tube design represents a good compromise between electrical yield, thermal yield, and manufacturability as the unglazed PVT collector gives the highest electrical efficiency, but its thermal performance is very poor.

A PVT water heater was analysed by Garg et al. (1994) and it was found that the thermal and electrical efficiencies of the hybrid solar water heater were 33.5% and 3.35%, respectively. Kim et al (2014) analysed the performance of a building heating system combined with a water-type unglazed PVT collector integrated into the roof of an experimental unit. According to the results, the electrical efficiency showed a high performance level of more than 16% while the heating system with the BIPVT collector was running. The water temperature of the thermal storage tank rose by 40° making it a viable heat source for heating.

In order to evaluate the performance of an unglazed flat-plate PVT compared to its power supply, a finite element heat flux simulation was performed and contrasted with a theoretical mathematical model. Therefore, a correlation between the energy absorbed by water within the pipes in the PVT panel and its inlet temperature is approximated.

The heat transfer analysis was performed to evaluate the thermal energy absorption of the water, the heat source being the residual heat from the solar cells. This analysis had several aims: to evaluate whether it is sufficient to achieve minimum water temperature for domestic hot water, the impact of the inlet water temperature on the thermal absorption of the water and its impact on the electrical efficiency of the solar cells.

2 Methodology

A moment-in-time heat flux analysis of an unglazed water-type flat-plate PVT panel was conducted by finite element modelling in ANSYS-FLUENT 14.0. Three different suppositions were studied: autumn equinox (AE) and summer and winter solstice (SS and WS), as representing the climatic

conditions over a whole year. The fundamental heat transfer governing equations were applied. The heat flux analysis is focused on the photovoltaic panel, the cooper plate absorber, the water pipes and the thermal insulation. Heat flux, both to outside air and to the water inside the pipes, is modelled by transference coefficients and are defined as boundary conditions. A steady-state approach is considered due to the shorter characteristic time of the transitory effects associated with heat accumulation in terms of environmental variation.

However, performing a Finite Element Analysis (FEA) does not produce a general closed-form solution which would enable the system's to respond to changes in various parameters to be examined. A mathematical model which could provide relatively quick results was created in order to obtain an analytical expression correlating temperature and water heat absorption.

For each case, results are obtained by simulation and by solving the analytical models. The difference between them is used to estimate the degree of freedom introduced. The analytical model, once validated, is solved for different inlet water temperatures.

Most of the results and procedures described can be extrapolated, although there are some starting determinants, which are important to bear in mind, especially the panel slope (8º) and the local climatic conditions and location.

3 Model description

The system consists of eight south-facing unglazed flat-plate PVT for domestic hot water heating (DHW) installed with an 8º gradient onto the roof of a solar house located in Madrid (40.24N, 3.41O) with no surrounding obstacles. The PVT collectors are connected to a 200-l storage tank. The PV sub-system is a grid-connected PV system. The PV laminates are connected to a PV inverter, converting the DC current into AC current. The PVT system layout is shown in Figure 1.

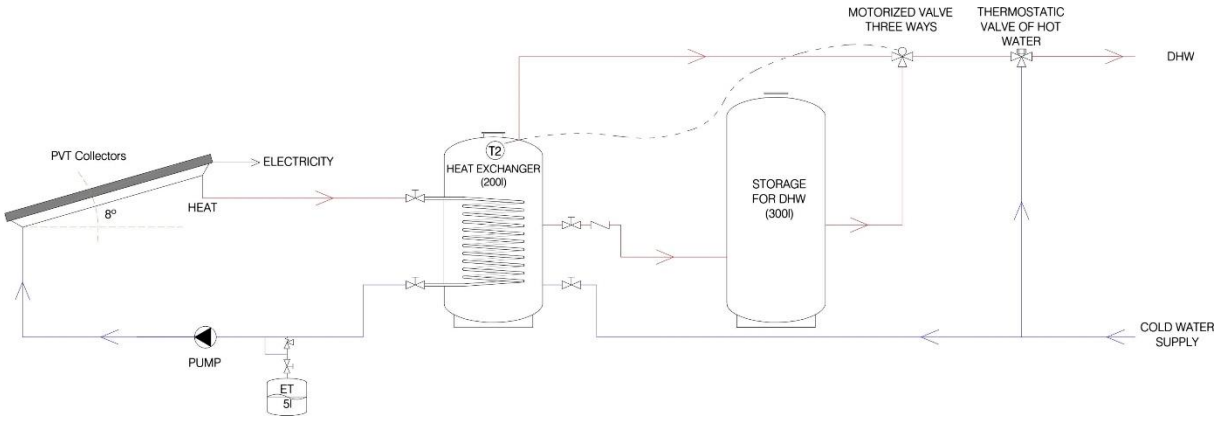

Figure 1: Schematic overview of the PVT system for domestic hot water.

The water-type unglazed PVT collector studied consists of a monocrystalline silicon PV panel and a water pipe circuit behind, in which a water-based HTF circulates and absorbs heat from the PV cells. A copper plate absorber is placed between the PV module and the water-pipe circuit, behind the PV cells and soldered onto the water pipes, which are also copper. The whole system is enclosed in a casing with thermal insulation on the rear and on the sides.

There are eight pipes per module, distributed in two groups. The distance between each pipe within a group is about 10 cm, leaving a distance of around 20 cm between each group, as shown in Figure 2. The water inlet and outlet ends were located at the lower and upper headers, respectively, allowing a balanced water flow in all pipes.

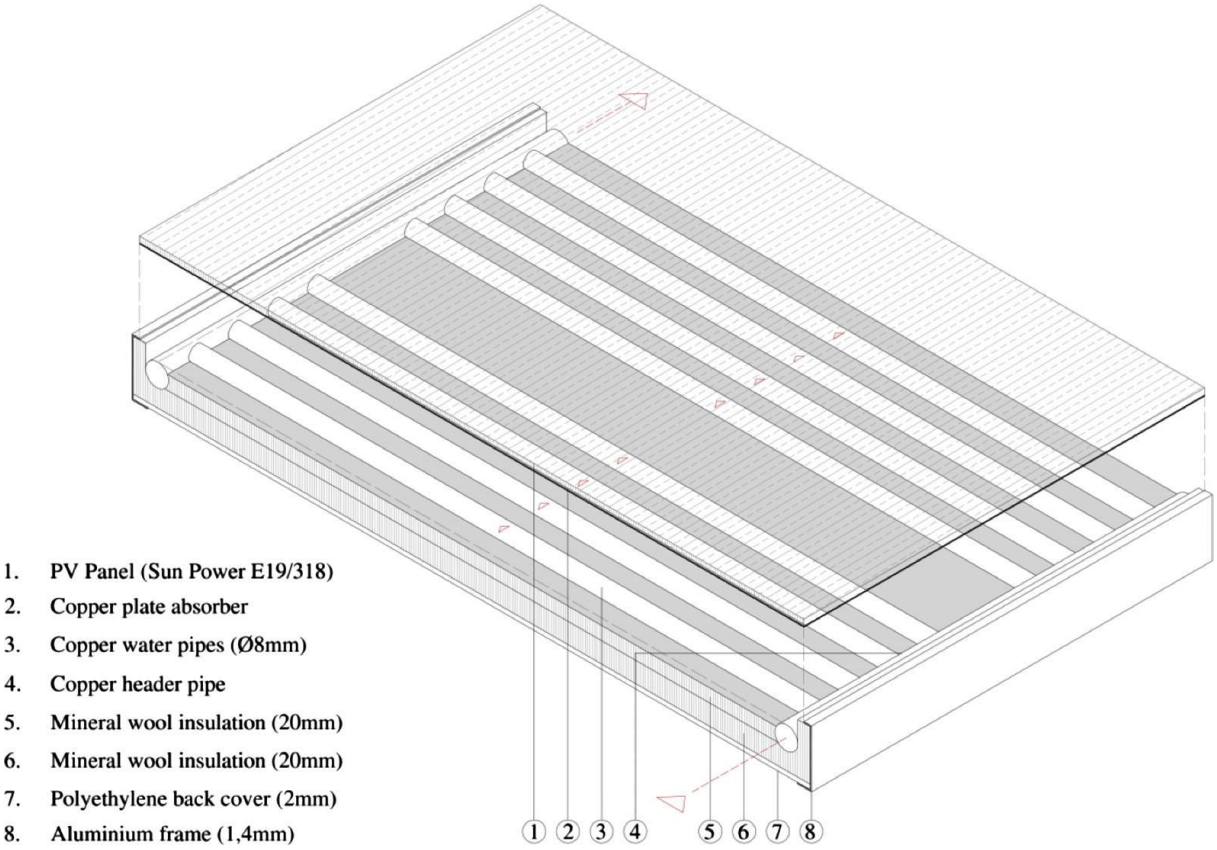

Figure 2: Unglazed water-type PVT collector

3.1 Calculation domain

To specify the calculation domain some hypotheses and simplifications were made. Firstly, the effect of the header pipes were obviated as, compared to the whole panel, it would affect only a small volume. In addition, considering that:

- the inlet and outlet water temperature difference at the water pipes is, at most, in the same order of the temperature difference occurring at the cross-section of the panel
- the length of the water pipe is much greater than the distance between water pipes,

It may be deduced that the longitudinal gradient of temperatures is going to be much less than the transverse and consequently, the problem can be considered as two-dimensional and the domain of calculus becomes a cross-section of the panel (Figure 3)

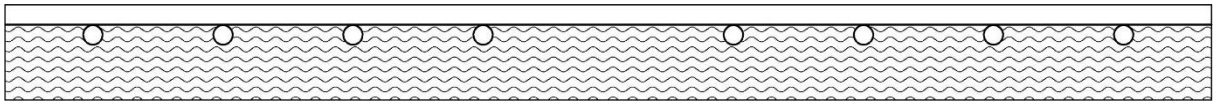

Figure 3: PVT cross section

It is understood that the temperature of all the water pipes is going to be very similar, so it is considered that there is one plane of symmetry coinciding with the axis of each water pipe and another with each inter-axis (Figure 4). In this way, we could extrapolate similar results for the whole panel from the results obtained for a water pipe and the region covered between two planes of symmetry.

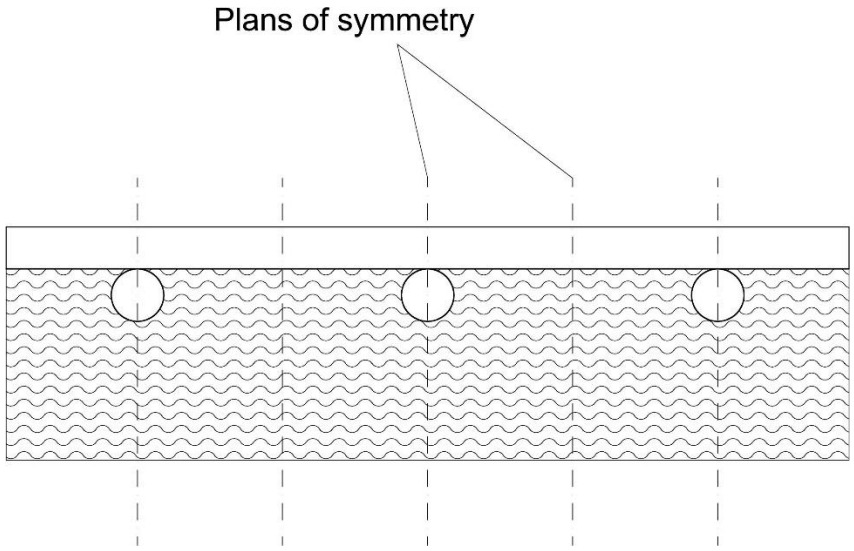

Figure 4: Plans of symmetry throughout the PVT cross section

The calculation domain resulting under these hypotheses is shown in figure 5.

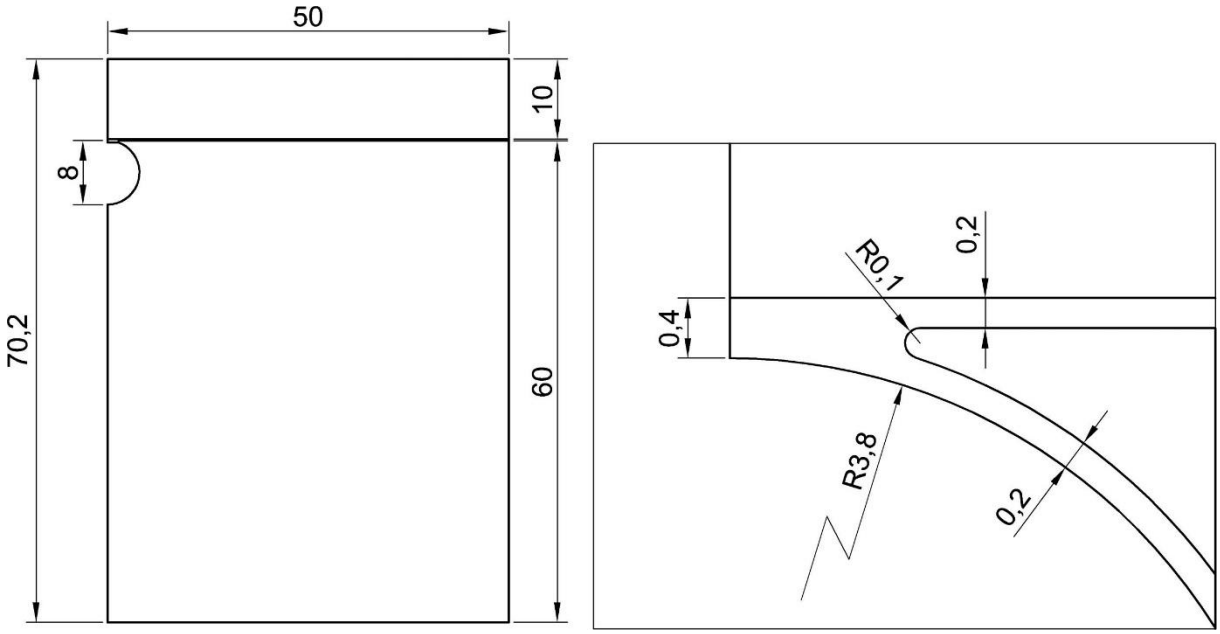

Figure 5: Dimensions and detail of the calculation domain (dimension marks in mm).

The copper plate absorber and copper water pipes have the same 0.2 mm thickness and they are soldered forming a 0.1-mmradius.

The material properties are shown in Table 1 and the HTF inside pipes is water, whose properties are shown in Table 2.

Solid Body	PVT panel	Absorber & Water pipes	Thermal insulation
Material	Laminated glass	Cooper	Mineral wool
Density [ρ] (kg/m^3)	2500	8933	50
Specific heat capacity [cp] (J/kg K)	750	385	670
Thermal conductivity [λ] (W/m K)	1,4	401,0	0,04

Table 1: Properties of solid bodies

Property	Value
Density [ρ] (kg/m^3)	997,0
Specific heat capacity [cp] (J/kg K)	4181,7
Thermal conductivity [λ] (W/m K)	0,6069
Dynamic viscosity [μ] (kg/m s)	8,899 x 10^{-4}
Prandtl Number [Pr]	6,1316

Table 2: Water properties

3.2 Environmental data

Supposing a clear sky, the hybrid panels were studied at noon and on three different dates: the autumn equinox as being representative of yearly average conditions, and the summer and winter

solstices. This serves to evaluate the panels' performance under extreme yearly conditions. A standardised weather file (*.wea) for Madrid, Spain (40.24N, 3.41O), is taken as source data for the hourly ambient temperature and incident solar radiation used in each calculated scenario.

In order to obtain more reliable results, the values used in simulations are averaged from the four central hours of the day, from 10:00 h to 13:00 h. The incidence angle of the Sun is calculated considering the angle of local latitude, the declination angle at noon and the slope of the panel, 8º from the horizontal plane. The data of mains water temperature for these days are also obtained.

The average environmental data obtained are shown in Table 3.

Magnitude	Summer solstice	Autumn Equinox	Winter solstice
Global solar radiation [G] (W/m^2)	1014	915	846
Diffuse solar radiation [D] (W/m^2)	168	145	93
Direct solar radiation [B] (W/m^2)	846	770	753
Sun angle of incidence [θ] (º)	17,05	40,5	63,95
Outside air temperature [Tout] (ºC)	27,53	25,37	6,64
Mains water temperature [Tw,0] (ºC)	12	10	8

Table 3: Input Climatic conditions data

4 Modelling

4.1 Finite element model

A simulation of the hybrid panel was performed with the aid of commercial FEM software in order to assess the heat transfer between the solid bodies of the PVT panel, the solar cells acting a heat source for the heat transfer to the copper water pipe and thence to the fluid flowing inside the pipe.

The calculation domain has been discretized into finite elements by means of a hexahedral mesh structured for the PV panel (1040 elements); the absorber and the water pipe (432 elements); and non-structured for the insulation (917 elements), resulting in a 2389-finite-element mesh (Figure 6).

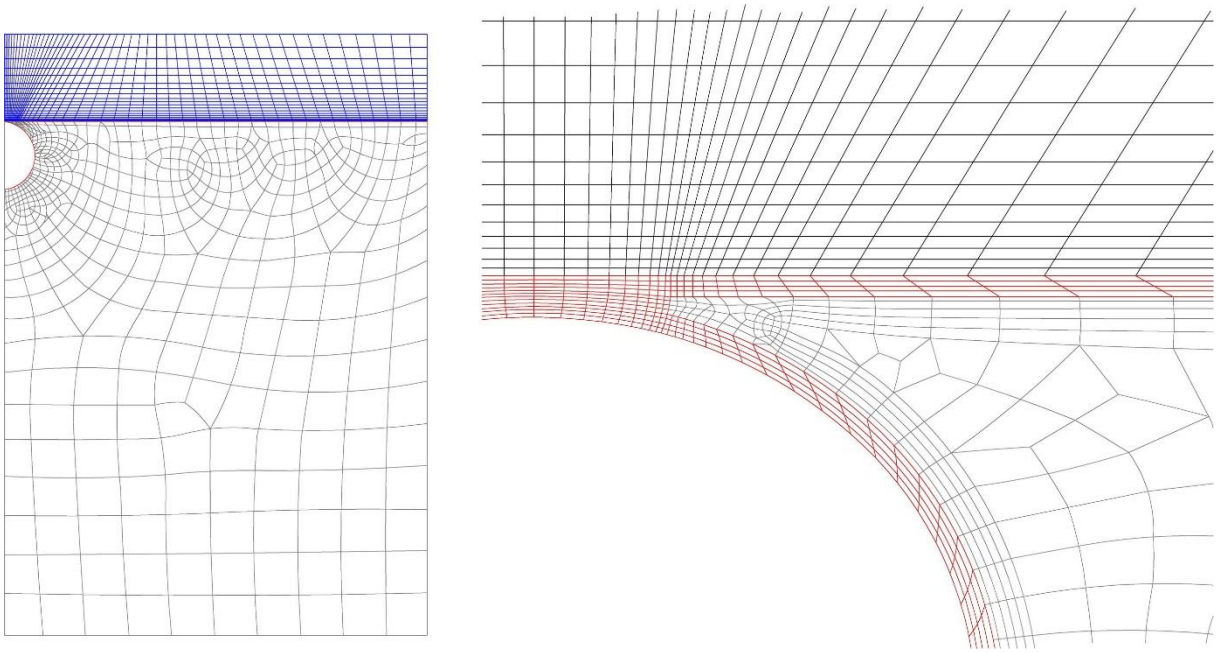

Figure 6: Simulation domain mesh. General and detailed view

This mesh has been refined in the water pipe and the absorber so there are at least four elements through the thickness and in its surroundings in order to appreciate the temperature gradients. All of the equations that have been used are described in Table 4.

Equation	Formula	
Thermal energy conservation	$q_x = -\lambda\, dT/dx$ where qx is the heat flux in the x direction (W/m^2); λ is the thermal conductivity (W/m K) and dT/dx is the temperature gradient (K/m)	(1)
Heat source (contact surface between the pv panel and the plate absorber)	$S = G - E - V$ where S is the heat source in the contact surface between the PV panel and the absorber (W/m^2); G is the incident global solar radiation over the PVT panel (W/m^2); E is the radiative heat flux on the photovoltaic cells surface (W/m^2) and V is the photovoltaic electric energy generation (W/m^2)	(2)
Incident global solar radiation over the photovoltaic cells	$G = D + B\cos(\theta - \beta)$ where D and B are the diffuse and direct solar radiations; this last one depends on the angle of incidence of the solar rays (θ) in the panels and the slope angle of the panel (β)	(3)
Emit radiation by cells in function of its temperature	$E = \varepsilon\sigma T^4$ where ε is the photovoltaic cells emissivity (ε = 1), σ is the Stefan–Boltzmann constant (5669 × 10^{-8} W/m^2 K^4) and T is the absolute cells surface temperature (K)	(4)
Electricity generated in output of a photovoltaic	$V = rGP_R$ where r is the solar panel yield given by the ratio of the electrical power of one solar panel divided by the area of	(5)

	one panel and PR is the performance ratio of the installation independently of the orientation and inclination of the panel and includes all losses	
Convective heat transfer	$$q = h(T_s - T_f)$$ where q is the convective heat flux (W/m^2); (Ts − Tf) is the temperature difference between the solid and the fluid and h is the convection heat transfer coefficient, (W/m^2 K)	(6)
Water flow	$$h_w = Nu_d \lambda / d$$ the hw coefficient is determined according to Nusselt number, Nu_d, and the internal pipe diameter (d = 7.6 mm)	(7)
Sieder and Tate expression	$$Nu_d = 1{,}86[Re_d Pr\, d/L]^{\frac{1}{3}}$$ where L is the length of the pipe (mm), Re_d is, and Pr is the Prandtl number. The equation is valid for 0.48 < Pr < 16,700 and (d/L)Re_dPr > 10	(8)
Reynolds number of the water flow	$$Re_d = 4m/\pi d\mu$$ being Re_d = 782.06 for m = 0.004154 kg/s (15 l/h), hw = 430.2 W/m^2 K	(9)
In each differential element, there is an exchange of heat by conduction qx and qx + dx with the adjacent elements	$$q_x = -ek\, dT/dx|_x$$ $$q_{x+dx} = -ek\, dT/dx|_{x+dx}$$	(10)
Upward convective heat flux	$$q_1 = h_1(T_{abs} - T_{out})dx$$	(11)
Heat transference coefficient h_1 can be defined as the inverse of the conductive thermal resistances of the absorber and the upper PVT surface heat transference coefficient (h_u)	$$1/h_1 = e_p/\lambda_p + 1/h_u$$ where ep is the thickness of the panel (ep = 0.01 m); λp is the thermal conductivity of the panel (λp = 1.4 W/m K); and hu is the upper PVT surface heat transference coefficient (hu = 4 W/m^2 K)	(12)
Downwards heat flux	$$q_2 = h_2(T_{abs} - T_{out})dx$$	(13)
Heat transference coefficient h_2 can be defined as the inverse of the conductive thermal resistances of the absorber and the upper PVT surface heat transference coefficient (h_d)	$$1/h_2 = e_i/\lambda_i + 1/h_d$$ Where ei is the thickness of the insulation (e_i = 0.06 m); λ_i is the thermal conductivity of the insulation (λ_i = 0.04 W/m K); and h_d is the bottom PVT surface heat transference coefficient (h_d = 2 W/m^2 K)	(14)
Differential equation for controlling the temperature of the copper plate absorber	$$ek\, d^2T/dx^2 - (h_1 + h_2)(T_{abs} - T_{out}) + S = 0$$	(15)
Absorber temperature (integrating the differential equation)	$$T_{abs} = T_{out} + S/(h_1 + h_2) + C_1 \cosh(ax)$$ where $a^2 = (h_1 + h_2)/ek$ and C1 are integral constants	(16)
Heat conduction in adjacent elements is analogous to the case of the copper plate absorber	$$q_l = -ek\, dT/dl|_l$$ $$q_{l+dl} = -ek\, dT/dl|_{l+dl}$$	(17)

Heat transfer to water by convection	$q_w = h_w(T_{wp} - T_w)dl$	(18)
Differential equation: neglecting the heat conduction through insulation, since its magnitude is expected to be much lower than heat flux through water pipe	$ek\, d^2T/dl^2 - h_w(T_{wp} - T_w) = 0$	(19)
Water pipe temperature imposing the adiabatic boundary condition at l = 0 and integrating the equation	$T_{wp} = T_w + C_2 \cosh(bx)$ Where $b^2 = h_w/ek$ and C2 are integral constants	(20)
Temperature and heat flux continuity has to take place at the junction point between the absorber and the water pipe	$T_{abs}(x = L/2) = T_{wp}(l = \pi\, d/2)$	(21)
	$ek\, dT/dx\|_{x=L/2} = -ek\, dT/dl\|_{l=\pi d/2}$	(22)
Based on these conditions C1 and C2	$C_2 = \dfrac{(a\, L/2 - T_w + S/h_1 + h_2)}{\left[\cosh(b\pi\, d/2) + (b \sinh\left(b\pi \frac{d}{2}\right)/a \sinh\left(a \frac{L}{2}\right))\right]}$	(23)
	$C_1 = -C_2\, b \sinh(b\pi d/2)/a \sinh(a\, L/2)$	(24)
Heat source value (as a function of the average absorber temperature, it is suppose that heat source is uniform)	$S(T_{av}) = G(1 - \eta(T_{av})) - \varepsilon\sigma T_{av}^4$	(25)
Average absorber temperature	$T_{av}(S) = \dfrac{1}{\frac{L}{2}} \int_0^{\frac{L}{2}} T(S,x)dx$ $= T_{out} + [S/(h_1 + h_2)] + \left[C_1 \sinh\left(\frac{aL}{2}\right) \Big/ \frac{aL}{2}\right]$	(26)
Part of the net heat flux from the heat source transferred to water	$W = S - (h_1 + h_2)(T_{av} - T_{out})$	(27)
Assuming that W is uniform along the water pipe, and given that the water pipes have a length Z of 1.5 m and L is the length of the circle describing the water pipe cross section	$LZW = m_w c_{p,w}(T_{w,out} - T_{w,in})$ Where, m is the water volume flow through each water pipe (m = 4154 10^{-3} kg/s); Tw,out is the outlet water temperature, and Tw,in is the inlet water temperature	(28)
Average water temperature	$T_{w,av}(S) = \frac{1}{2}(T_{w,out} + T_{w,in})$	(29

Table 4: Equations used in the modelling process

The heat conduction and heat accumulation in the hybrid panel solids were modelled considering the thermal energy conservation equation and Fourier's Law.

$$q_x = -\lambda\, dT/dx \quad (1)$$

It is assumed that PV panel glass is perfectly transparent and that both the copper bodies and the insulation are opaque, black surfaces and diffused surfaces. The part of the global solar irradiation that is neither reflected by the cell nor converted to electricity is considered as the heat source (*S*) in the contact surface between the PV panel and the plate absorber and can be defined as:

$$S = G - E - V \tag{2}$$

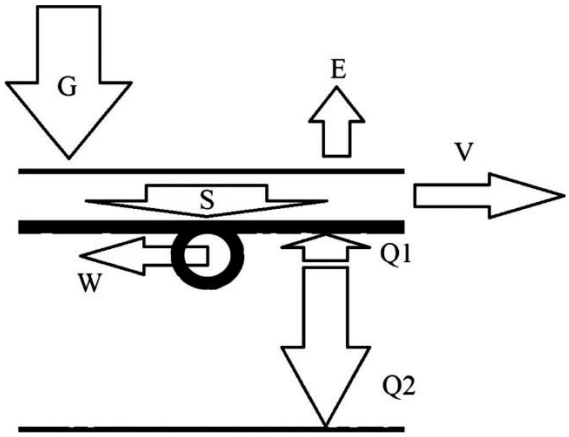

Figure 7: Schematic heat fluxes

The diffuse (D) and direct (B) solar radiations compose the incident global solar radiation over the photovoltaic cells; this latter depends on the solar rays' angle of incidence (ϑ)on the panels and the gradient of the panel (β):

$$G = D + B\cos(\theta - \beta) \tag{3}$$

On the other hand, the surface of the cells will emit radiation in function of its temperature, given by the Stefan–Boltzmann Law:

$$E = \varepsilon\sigma T^4 \tag{4}$$

The global formula to estimate the electricity generated in the output of a photovoltaic system is:

$$V = rGP_R \tag{5}$$

The averaged environmental data for the autumn equinox and summer and winter solstices are the initial environmental conditions. Initial inlet water temperature ($T_{w\,in}$) at PVT panel is assumed to be equal to inlet water temperature at the storage tank, in other words, it is equal to the mains water temperature ($T_{w,0}$). Heat dissipation towards the environment by radiation and convection and heat transfer by convection to water are defined as boundary conditions.

On those boundaries coincident with the problem symmetry axis, adiabatic boundary condition is imposed (q=0). In the rest of the problem, heat transmission between the surface of a solid body

and the surrounding fluid media is modelled by the equation for convective heat transfer, given by Newton's law of cooling as:

$$q = h(T_s - T_f) \tag{6}$$

Two kinds of boundaries can be identified within this performance: heat transference between surfaces in contact with outside air and heat transference between internal water pipes' surface and the HTF.

Heat transference coefficient for the PVT panel lower surface (*h1*) includes heat transferred to the environment by convection and radiation, while the upper surface coefficient (*h2*) includes heat evacuation by convection as it is transparent. Heat exchange due to radiation, crossing the upper face of the PVT panel, takes place on the internal surface of the cell, and it has been already considered in the heat source (*S*). Both values, h1 and h2, were calculated based on simulations of the photovoltaic panels. In both cases, the fluid temperature (T_f) is the outside air temperature (T_{out}).

The lower PVT surface heat transference coefficient (h_b) was calculated by obtaining the ratio between the heat transferred downward by convection and radiation and the temperature gradient between the surface and the outside air (approximately 2 W/m^2 K). Upper PVT surface heat transference coefficient (h_u) was calculated by obtaining the ratio between the upward heat transferred by convection and the temperature difference between the upper surface of the panels and the outside are (approximately 4 W/m^2 K).

In order to determine the heat transference between internal water-pipes surface and the water flow (h_w), correlations are employed for forced convection within pipes.

$$h_w = Nu_d \lambda / d \tag{7}$$

Supposing a 120 l/h water flow through the header pipes, in other words, 15 l/h water flow per pipe, the internal water flow could be considered laminar. On the other hand, the effects of the entrance region cannot be ignored since the water pipes are not large enough. For these cases, the Sieder and Tate expression is usually employed. If the temperature dependence of the water viscosity is not taken into consideration:

$$Nu_d = 1{,}86[Re_d Pr\, d/L]^{1/3} \tag{8}$$

The Reynolds number of the water flow inside the water pipe depends on the thickness of the copper plate absorber, the mass flow rate (m) and the dynamic viscosity (μ):

$$Re_d = 4m/\pi d\mu \tag{9}$$

Fluid temperature would be the average water temperature inside the pipe.

4.2 Mathematical Model

It is possible to obtain an approximate analytical solution to the heat conduction problem in the absorber and the water pipe. As the absorber length and the pipe cross-section are much larger than their thickness, the problem can be considered as being unidirectional. The analytical model solves the unidirectional heat equation in both absorber and water pipe, simplifying the heat transference in the other solid bodies.

The calculation domain of the absorber and water pipe is shown in Figure 8. Thermal conductivity λ and thickness e are known, while the longitude of the absorber x and of the pipe l are the variables.

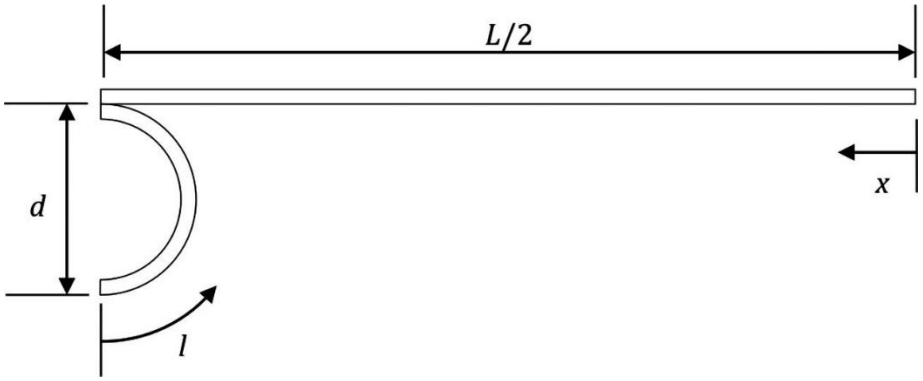

Figure 8: Length variables sketch over the calculation domain

4.2.1 Copper plate absorber

The energy balance in a differential element of the copper plate absorber is represented in Figure 9.

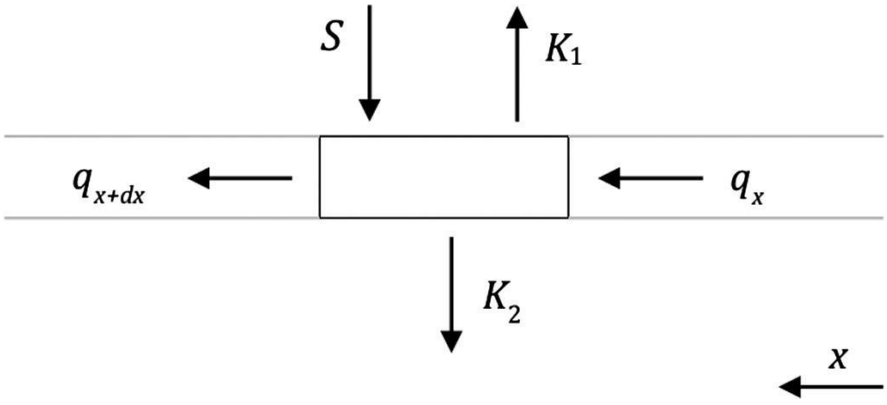

Figure 9: Energy balance in a copper plate absorber differential element

In each differential element, there is an exchange of heat by conduction qx and $qx+dx$ with the adjacent elements that are defined according to the expression:

$$q_x = -ek\,dT/dx|_x;\ q_{x+dx} = -ek\,dT/dx|_{x+dx} \quad (10)$$

On the other hand, each element will receive a net heat contribution from the heat source $S \cdot dx$, which results from the incident global solar radiation, the emission of radiation and the electricity generation (Equation 1). Although this heat source depends on the temperature and, therefore, it will be different for each element of the copper plate absorber, this simplification supposes it to take a uniform value for all of the points in the copper plate absorber's differential elements.

There will be an upward convective heat flux q_1, to be conducted through the PV cell, dissipated into the environment by convection on the upper side, which can be assumed to be proportional to the temperature gradient between the absorber temperature and the outside air temperature:

$$q_1 = h_1(T_{abs} - T_{out})dx \quad (11)$$

Heat transference coefficient $h1$ can be defined as the inverse of the conductive thermal resistances of the absorber and the upper PVT surface heat transference coefficient (h_u):

$$1/h_1 = e_p/\lambda_p + 1/h_u \quad (12)$$

Similarly, a downward heat flux q_2 will take place. This will be driven through the insulation and dissipated to the outside air:

$$q_2 = h_2(T_{abs} - T_{out})dx \quad (13)$$

Coefficient h_2 being:

$$1/h_2 = e_i/\lambda_i + 1/h_d \quad (14)$$

Upwards, the thermal conduction resistance of the absorber is much lower than that of convection; downwards, the heat transfer is small compared to conduction in the absorber so that its influence on the energy balance is limited. Therefore, the error introduced by both approaches is acceptable.

To summarise, the temperature of the copper plate absorber will be controlled by the differential equation:

$$ek\,d^2T/dx^2 - (h_1 + h_2)(T_{abs} - T_{out}) + S = 0 \quad (15)$$

Imposing the adiabatic boundary condition at $x = 0$ and integrating the differential equation, the absorber temperature can be expressed as follows:

$$T_{abs} = T_{out} + S/(h_1 + h_2) + C_1\cosh(ax) \quad (16)$$

Where $a^2 = \frac{h_1+h_2}{ek}$ and C_1 are integral constants.

4.2.2 Water pipe

In the case of the water pipe, whose thickness is much smaller than its diameter, the effects of its curvature can be obviated and we consider instead a cross-section of the water pipe as a straight element whose length is $\pi d/2$. The energy balance in a differential element of the water pipe is shown in Figure 10.

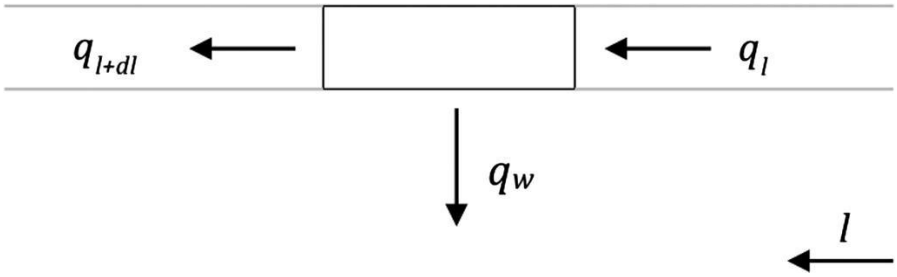

Figure 10: Energy balance in a water pipe differential element

Heat conduction in adjacent elements is analogous to the case of the copper plate absorber (equation 10).

$$q_l = -ek\, dT/dl|_l;\ q_{l+dl} = -ek\, dT/dl|_{l+dl} \tag{17}$$

At each element the difference of the conducted heat is due to the heat transfer to water by convection (q_w), which can be assumed as being proportional to the temperature gradient between the water pipe temperature and the water temperature, h_w being the internal water pipe heat transference coefficient:

$$q_w = h_w(T_{wp} - T_w)dl \tag{18}$$

In this case, a simplification was assumed and heat conduction through insulation was dismissed, since its magnitude is expected to be much lower than heat flux through the water pipe. The resulting differential equation is:

$$ek\, d^2T/dl^2 - h_w(T_{wp} - T_w) = 0 \tag{19}$$

Imposing the adiabatic boundary condition at $l=0$ and integrating the equation, the water pipe temperature can be expressed as follows:

$$T_{wp} = T_w + C_2 \cosh(bx) \tag{20}$$

Where $b^2 = h_w/ek$ and C_2 are integral constants.

4.2.3 Closed-form solution

Temperature and heat flux continuity has to take place at the junction point between the absorber and the water pipe, which can be expressed by a closed-form solution:

$$T_{abs}(x = L/2) = T_{wp}(l = \pi\, d/2) \tag{21}$$

$$ek\, dT/dx|_{x=L/2} = -ek\, dT/dl|_{l=\pi d/2} \tag{22}$$

Based on these conditions, C_1 and C_2 can be obtained following these equations:

$$C_2 = (a\, L/2 - T_w + S/h_1 + h_2)/[\cosh(b\pi\, d/2) + (b \sinh(b\pi\, d/2)/a \sinh(a\, L/2))] \tag{23}$$

$$C_1 = -C_2\, b \sinh(b\pi d/2)/a \sinh(a\, L/2) \tag{24}$$

All the parameters involved in the closed-form solution are constant, except for the heat source value S, which can be approximated as a function of the average absorber temperature T_{av} as it is supposed that the heat source is uniform:

$$S(T_{av}) = G\big(1 - \eta(T_{av})\big) - \varepsilon\sigma T_{av}^4 \tag{25}$$

Furthermore, the average absorber temperature is described by:

$$T_{av}(S) = \frac{1}{L/2}\int_0^{L/2} T(S,x)dx = T_{out} + [S/(h_1 + h_2)] + [C_1 \sinh(aL/2)/aL/2] \tag{26}$$

The water temperature problem can be solved for either specific value, requiring an intake temperature of water and considering its heating along the pipe in order to calculate an average value. This latter was the chosen approach.

By analysing the energy balance in the absorber, it can be concluded that part of the net heat flux from the heat source S is dissipated by conduction through the PV panel and insulation layers to the environment and the other part is transferred to water (W):

$$W = S - (h_1 + h_2)(T_{av} - T_{out}) \tag{27}$$

Assuming that W is uniform along the water pipe, and given that the water pipes have a length Z of 1.5 m and L is the length of the circle describing the water pipe cross section:

$$LZW = m_w c_{p,w}\big(T_{w,out} - T_{w,in}\big) \tag{28}$$

If the heat flux to the water is uniform, the average water temperature $T_{w,av}$ in the water pipe will be:

$$T_{w,av}(S) = \frac{1}{2}\big(T_{w,out} + T_{w,in}\big) \tag{29}$$

This system of equations can be solved by means of an iterative method: from an initial estimation of S and of T_w, T_{av} (S, T_w) is calculated and with that result, the new values of S and T_w are obtained (S', T'_w). The process is repeated until the numerical values remain steady.

5 Results

5.1 Comparison between simulation and mathematical model

For each case studied, the problem has been solved by means of both finite element simulation and by an analytical model, considering that the inlet water temperature is the same as the mains water temperature. Simulation provides a more reliable solution, but the mathematical model allows results to be obtained quickly.

In the three cases, both methods' results are very similar. Therefore, once the validity of the analytical method is proven, taking into account the similarity of the results obtained, this method has been employed to solve the problem when given different inlet water temperatures. This gives a wider perception of the performance of the panel under different operating conditions.

The environmental data used are taken from Table 3 where the resulting average water temperature for each case can be observed. Temperature distribution in the cross-section of the PVT panel obtained by simulation and temperatures referring to position (m) on the upper surface of the absorber, in contact with PV cells, and on the internal surface of the water pipe, calculated by simulation and equations are shown for each case in Figures 11 and 12 respectively.

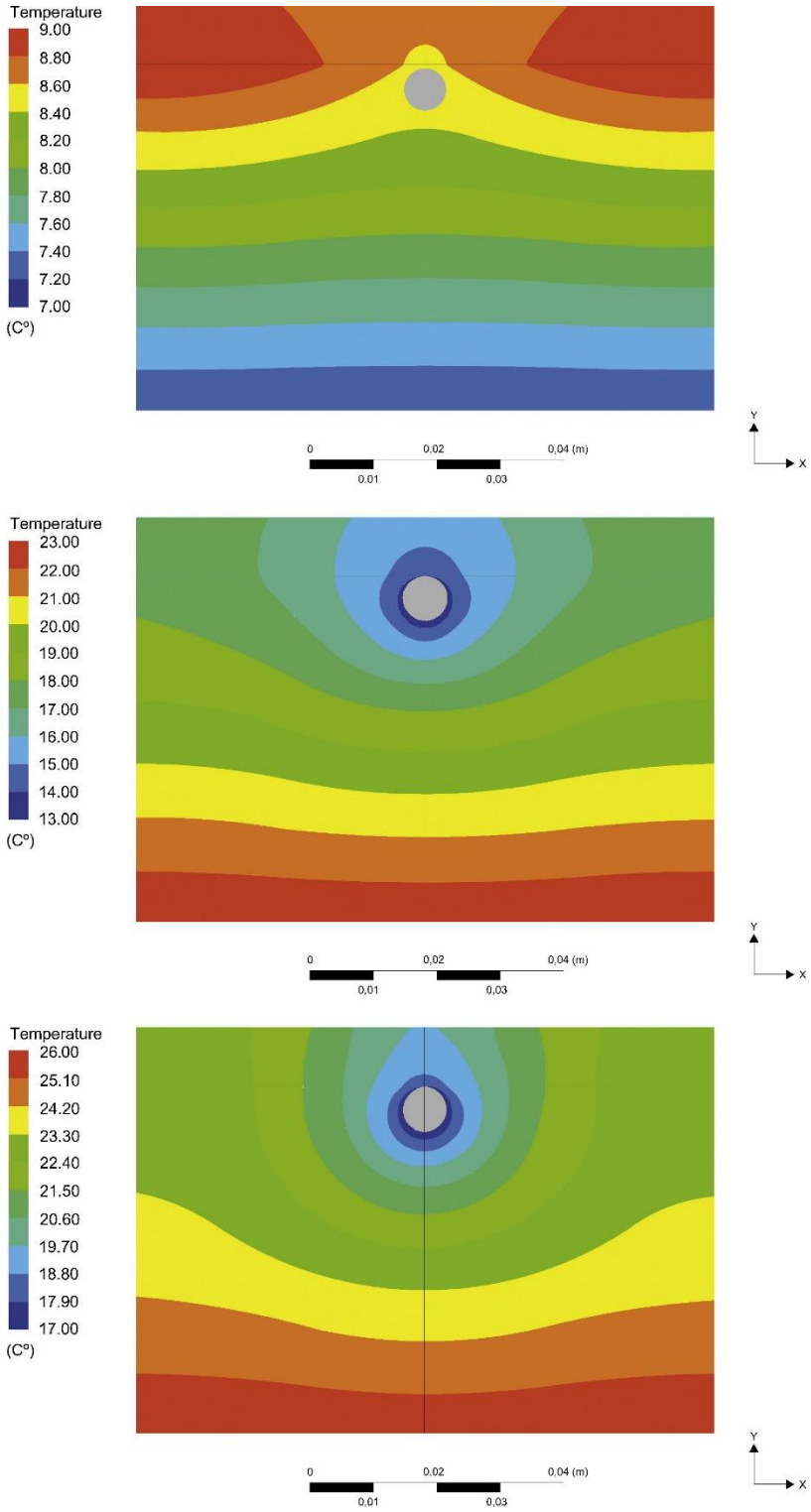

Figure 11: Temperature distribution in the cross-section of the PVT panel obtained by simulation

The temperature distributions for both summer solstice and autumn equinox are shown to be similar, while the winter solstice presents an important difference. The summer solstice temperature distribution reaches a higher temperature at the lower part side of the panel than autumn equinox

temperature distribution. Moreover, its temperature gradient is less homogeneous at the outer surface of the PV cells than during the equinox, the temperature range being 18-23°C at the absorber during summer solstice and 15-18°C during the autumn equinox. Despite these differences, and considering a similar behaviour for both spring and autumn equinox, the PVT panel can guarantee a reasonably good performance for at least six months. During the winter solstice, the temperature difference is as low as 2°C, so there is no appreciable difference in the temperature distribution, resulting in a homogeneous performance.

For both summer solstices and equinoxes, the outside temperature is much higher than the average water temperature, having a difference of around 15°C. The water flowing through the pipes absorbs part of the heat produced by PV cells, improving their performance as well as reducing auxiliary DHW energy consumption. During winter solstice, the water flowing through the pipes has a higher temperature than the PV cells, transferring heat to them. These cells have a higher temperature than the lower part of the PVT panel and the outside temperature.

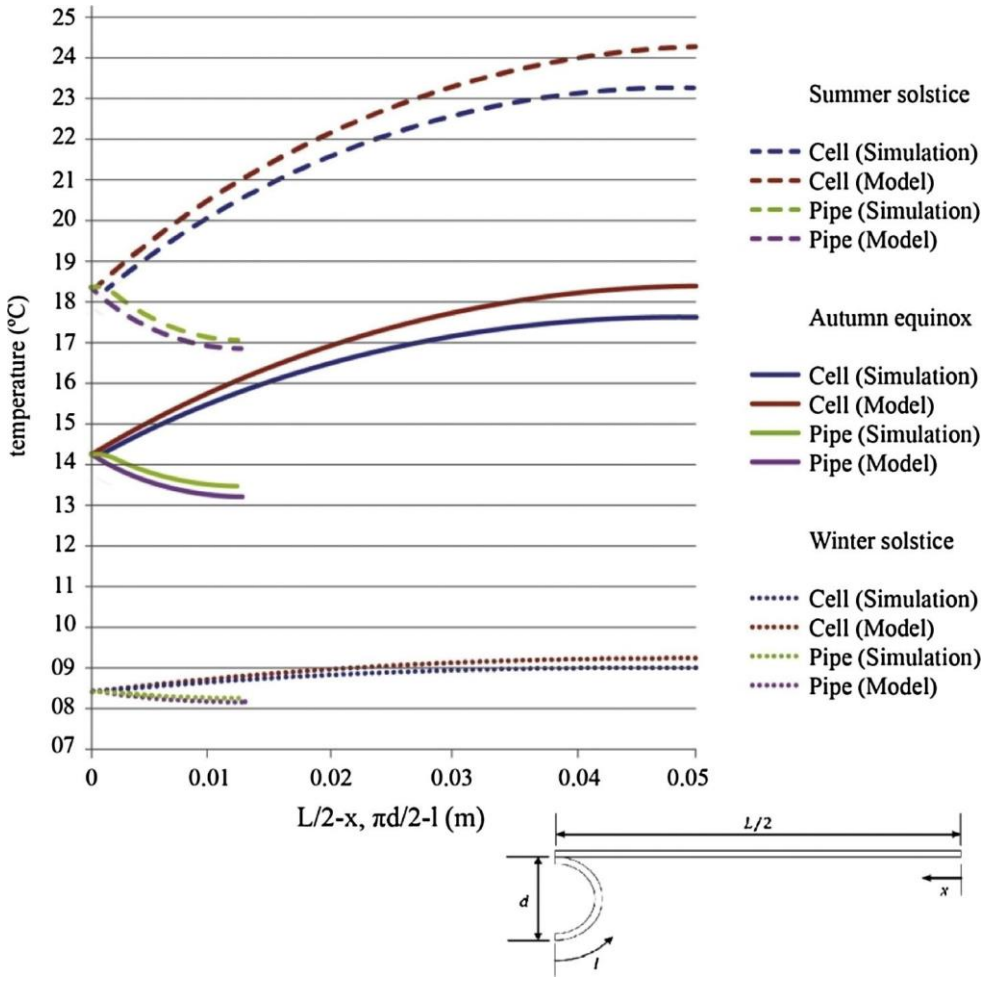

Figure 12: Temperature of the copper plate (cell) and of the water pipe referring to position (m)

For every analytical model, the results are slightly higher than the simulation results. Nevertheless, the analytical model and the simulations provide very similar temperature values at the contact point, but from there on, the analytical model presents greater gradients of temperature on the opposite sides of the water pipe and of the copper plate absorber.

The energy balance results that are obtained by both methods are presented in Table 5 and Figure 13. It can be observed how during summer solstice and autumn equinox, W is higher than S and Q1 and Q2 are negative, indicating that water through pipes absorbs heat from the closed environment, but for the winter solstice this behaviour is inversed.

	Summer Solstice			Autumn Equinox			Winter Solstice		
Magnitude	Simulation	Model	Δ	Simulation	Model	Δ	Simulation	Model	Δ
G (W/m²)	1003.47	1003.47	0.00	794.41	794.41	0.00	514.62	514.62	0.00
E (W/m²)	427.78	431.78	4.00	398.94	401.72	2.78	358.58	358.79	0.21
V (W/m²)	207.39	206.84	-0.55	167.32	167.00	-0.32	111.43	111.41	-0.02
S (W/m²)	368.30	364.85	3.45	228.15	225.69	2.47	44.61	44.42	0.19
Q1 (W/m²)	-23.21	-20.51	-2.70	-34.63	-32.65	-1.99	8.58	8.76	-0.18
Q2 (W/m²)	-3.40	-2.64	-0.77	-4.80	-4.20	-0.60	1.10	1.13	-0.02
W (W/m²)	394.86	389.48	5.38	267.62	264.89	2.73	34.92	33.60	1.03
Tabs (°C)	21.55	22.26	-0.70	16.46	16.98	-0.51	8.85	8.89	-0.05
Twp (°C)	17.53	17.28	0.24	13.75	13.60	0.16	8.49	8.46	0.03

Table 5: Results for each calculation day, obtained by simulation and by the analytical method.

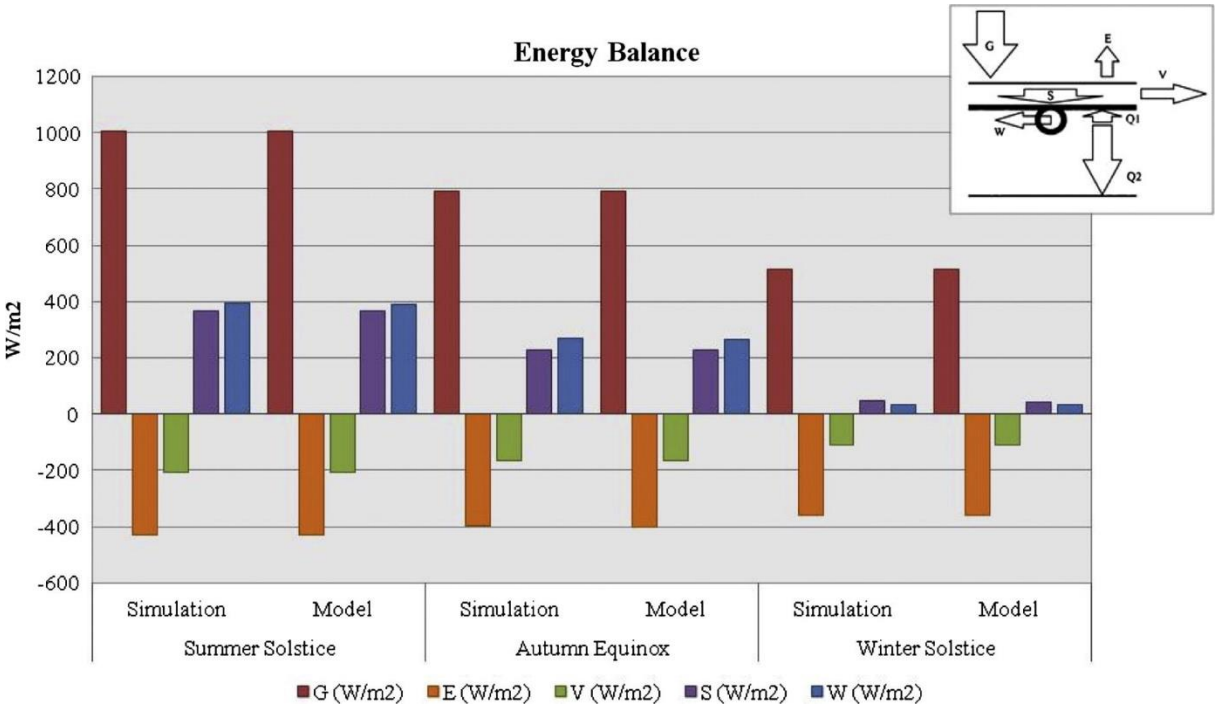

Figure 13: Energy Balance by simulation and the analytical model

Photovoltaic electric energy generation (V) and the radiative heat flux (E) are up to 20 and 40% of the incident global solar radiation (G) over the PVT panel, respectively. These percentages are kept in a linear relationship throughout the entire year, especially from one equinox to the other. This is not the case of the energy flux transferred to water (W), which does not maintain a linear relationship with the incident global solar radiation, sharply decreasing during the winter solstice.

The percentage of the incident global solar radiation over the PVT panel transferred to water is higher than the percentage of electrical energy generation, being up to 40-33% and 20-21% respectively during the summer solstice and autumn equinox. For the winter solstice, this percentage falls to 6.5%, affecting the global performance of the PVT panel. Furthermore, photovoltaic electrical energy generation in winter produces around half of that produced in summer, while the energy transferred to water is barely reaches 8% of the value obtained in summer.

Applying the analytical method presents very similar results to the simulation as regards the balance of energy. With respect to the temperatures, the differences are much greater, although they remain acceptable, with digressions near to 1%. Nonetheless, the analytical method gives less water warming than the simulation andcan, therefore, be defined as a conservative method.

5.2 Influence of inlet water temperature

The influence of inlet temperature water over the absorber and water pipe values are shown in Table 6 and represented in Figure 14 and 15.

	$T_{w,int}$ (°C)	$T_{w,out}$ (°C)	ΔT (°C)	T_{abs} (°C)	T_{wp} (°C)	S (W/m^2)	V (W/m^2)	W (W/m^2)
Summer solstice	12	15.36	3.36	22.26	17.28	364.85	206.84	389.48
	18	20.96	2.96	27.02	22.65	340.04	203.14	342.43
	24	26.54	2.54	31.75	27.99	313.99	199.46	294.29
	30	32.12	2.12	36.45	33.32	286.71	195.80	245.05
	36	37.68	1.68	41.13	38.64	258.18	192.16	194.68
	42	43.24	1.24	45.77	43.94	228.36	188.55	143.18
	48	48.78	0.78	50.38	49.23	197.26	184.96	90.54
	54	54.32	0.32	54.97	54.50	164.87	181.40	36.74
Autumn equinox	10	12.29	2.29	16.98	13.59	225.69	167.00	264.89
	15	16.95	1.95	20.96	18.07	205.62	164.55	226.23
	20	21.61	1.61	24.92	22.54	184.73	162.11	186.84
	25	26.27	1.27	28.86	26.99	163.01	159.68	146.70
	30	30.91	0.91	32.79	31.44	140.43	157.27	105.80
	35	35.55	0.55	36.69	35.87	117.00	154.86	64.14
	40	40.19	0.19	40.57	40.30	92.70	152.47	21.71
	42	42.04	0.04	42.12	42.06	82.73	151.52	4.52
Winter solstice	5	5.49	0.49	6.48	5.76	55.57	112.37	56.30
	6	6.42	0.42	7.29	6.66	51.88	112.05	48.86
	7	7.36	0.36	8.09	7.56	48.16	111.73	41.39

	8	8.29	0.29	8.89	8.46	44.42	111.41	33.90
	9	9.23	0.23	9.70	9.36	40.64	111.09	26.36
	10	10.16	0.16	10.50	10.26	36.83	110.79	18.83
	11	11.10	0.10	11.30	11.15	32.99	110.45	11.25
	12	12.03	0.03	12.10	12.05	29.12	110.13	3.64

Table6: Outlet and differential water temperature and temperature of the copper plate absorber and water pipe for each calculation day, obtained by the analytical model, and for different inlet water temperatures.

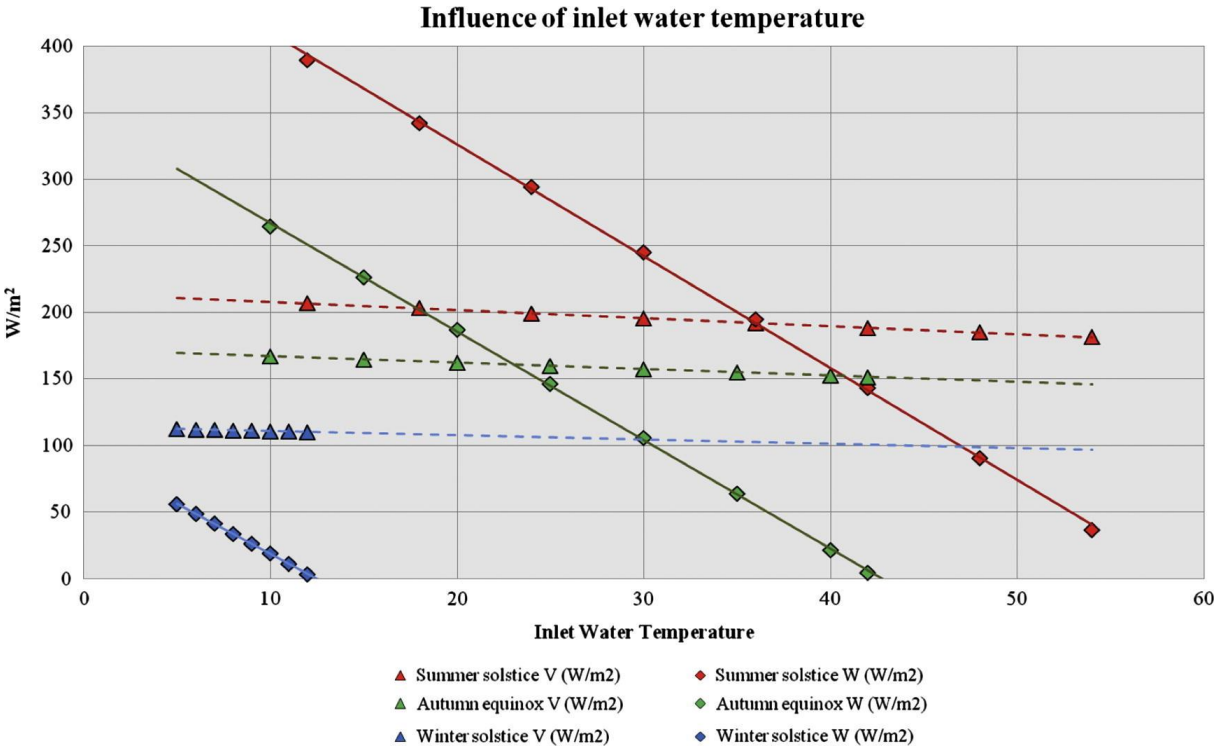

Figure 14: Energy fluxes (W/m²) due to inlet water temperature (ºC). Analytical model

The energy transferred in each inlet water cycle is highly constant throughout year. Despite this, the photovoltaic electrical energy generation presents small annual variations compared to W values. As is to be expected, the difference of water temperature ($T_{w,in}$ - $T_{w,out}$) is much higher in summer than in winter but after eight cycles the water temperature difference is of low influence.

Although $T_{w,out}$ hardly reaches 60°C, it can be observed that from spring to autumn equinox an outlet water temperature higher than 40°C is guaranteed. This is a sufficiently high DHW temperature for this period. In order to heat the water to be used during winter, auxiliary energy consumption would, in any case, be necessary. The photovoltaic performance could be compromised by the high water temperature in summer, especially if DHW consumption is insufficient, or if overheating occurs.

The net heat flux from the heat source S in the PVT panel transferred to water, W (W/m^2) depends on the inlet water temperature and can be approximated by a regression line:

$$W = (e - fT_{w,in}) \tag{30}$$

The values obtained for e, f and the coefficient of determination, R^2, for each case are shown in Table7.

	e	f	R^2
Summer solstice	494.17	8.3975	0.9995
Autumn equinox	348.68	8.1503	0.9997
Winter solstice	94.012	7.5229	1.00

Table 7: e, f, and R^2 for each scenario

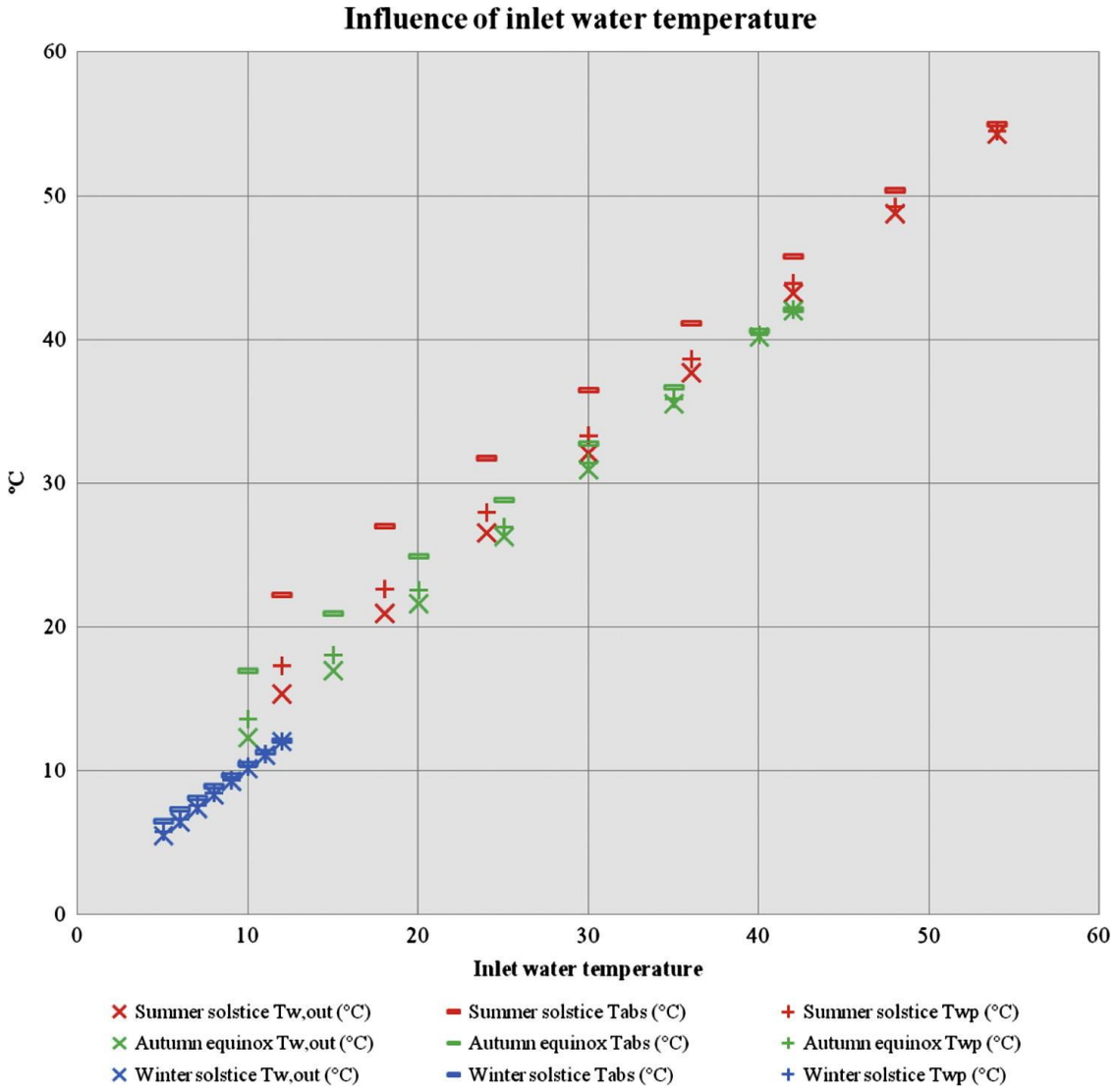

Figure 15: Outlet water, upper absorber surface and internal water pipe surface temperatures (°C) due to inlet water temperature (°C). Analytical model

As water temperature increases, the temperature of each other element converges. It is observed that after eight water cycles a situation close to thermal balance is achieved. For the first cycles, the difference from inlet to outlet water temperature is up to 0.5°C for the winter solstice, 2.3°C for the autumn equinox and 3.4°C for the summer solstice.

Electricity generation, however, decreases with the rise in water temperature. Given that the fall of efficiency with the rise in temperature is small, electricity generation could be considered constant.

The power that is finally transferred to the water falls heavily with its inlet temperature (considering that the water flow is constant). This means that, from a certain point onwards, the higher the water temperature is, the less the water is warmed. In other words, the panels are useful for warming water to a certain point, but from that point onwards, their efficiency is very low.

In any case, heat exchange contributions to the environment and to the water in the energy balance are small with respect to both the photovoltaic generation and to the cells' emission of radiation during the winter solstice.

6 Conclusions

This study has analysed the functioning of hybrid solar panels in different operating conditions. The results obtained from a comparative analysis of simulation results produced by finite element modelling and the calculation results obtained by analytical models demonstrate the possible difficulties and obstacles that may occur in each situation and during the different seasons of the year. These results validate both calculation processes as their values converged, the analytical models being more conservative as they gave higher absorber temperatures and lower water pipe temperatures than the finite element models.

These results show that, on a clear day, hybrid panels installed with an 8° gradient in Madrid provide all the necessary heat to cover the demand for DHW during the summer solstice and part of the demand during the autumnal equinox. During the winter solstice, however, the panels' contribution to heat generation is almost negligible. It must be borne in mind that the 8° inclination of the panels is far from optimal and it is detrimental to their efficiency during the winter season. The inclination of the cover should have been greater in order to optimise solar collection, having a value greater than the latitude of the location. Nonetheless, this inclination, imposed by building design, has been the optimal one during the equinoxes.

Despite this, the global thermal balance is positive: for the studied latitude, a PV cell would have an expected performance value of around 20%, but the PVT analysed panel achieves a performance up to 60% because of greater use of global incident solar radiation per square metre.

Global operation is negative during winter, as the water does not achieve an adequate temperature to be used, both increasing losses and decreasing the global performance of the system. However, it is optimal from one equinox to the other as water absorbs heat from the back of the PV cells, increasing their performance. One of the weakness of a PVT panel is that it is much more sensitive to an overproduction of thermal energy, especially in summer when there is a higher risk due to lower DHW consumption at a lower water temperature. This situation produces overheating in the PVT panel that decreases both the global performance and the system's lifetime. This problem could be solved by adding a heat sink at the top of the system.

The values obtained show that the temperature of the photovoltaic cells will depend greatly upon the temperature of the water in the water pipes. Hence, electrical efficiency will improve only if the temperature of the water is not very high. On the other hand, in the summer, once the DHW demand is covered and when there is no water flow, overheating problems can appear due to the insulation of the panel. Nonetheless, in such conditions the electrical efficiency is high.

During the Solar Decathlon Europe 2012 competition, the data provided from this research concluded that it was a favourable decision to include this kind of panels in one of the modules of the dwelling in order to provide a solution to the need for both hot water and electricity. The fact that our team won 1st prize in both Energy Evaluation and in Energy Efficiency team confirmed that it was indeed a good decision.

Acknowledgement

The authors would like to thank "Andalucía Team" for giving them the opportunity to participate in the Patio 2.12 project for the Solar Decathlon Europe 2012. The authors also would like to express our gratitude to Artesa (Aplicaciones Solares) S.A. for providing us with data from monitoring the PVT panels.

Funding

This research did not receive any specific grant from funding agencies in the public, commercial, or not-for-profit sectors.

References

Andalucia Team, 2012. Solar Decathlon Europe 2012.http://www.sdeurope.org/wp-content/pdf/AND_PD_7.pdf, may 2016.

Anderson, T. N., M. Duke, G. L. Morrison, and J. K. Carson, 2009. Performance of a building integrated photovoltaic/thermal (BIPVT) solar collector. Solar Energy, 83, 445-455.

Antonanzas, J., del Amo,A., Martinez-Gracia, A., Bayod-Rujula, A.A., Antonanzas-Torres, F., 2015. Towards the optimization of convective losses in photovoltaic–thermal panels. Solar Energy, 116, 323-336.

Buker, Mahmut Sami, Riffat, Saffa B., 2015. Building integrated solar thermal collectors - A review. Renewable and Sustainable Energy Reviews, 51, 327-346.

Chow, T.T., 2003. Performance analysis of photovoltaic-thermal collector by explicit dynamic model. Solar Energy, 75, 143-152.

ESTIF – European Solar Thermal Industry Federation, 2007. Solar Thermal Action Plan for Europe: Heating & Cooling from the Sun. Brussels: Renewable Energy House.

Garg, H. P., Agarwal, R. K., Joshi, J. C., 1994. Experimental study on a hybrid photovoltaic/thermal solar water heater and its performance predictions. Energy Conversion Management, 35, 621-633.

Kalogirou, Soteris A., 2001. Use of TRNSYS for modelling and simulation of a hybrid pv–thermal solar system for Cyprus. Renewable Energy, 23, 247-260.

Kim, J.H., Park, S.H., Kang,J.G., Kim, J.T., 2014. Experimental performance of heating system with building integrated PVT (BIPVT) collector. Energy Procedia, 48, 1374-1384.

Kumar, A., Baredar,P., Qureshi, U., 2015. Historical and recent development of photovoltaic thermal (PVT) technologies. Renewable and Sustainable Energy Reviews, 42, 1428-1436.

Santbergen, R., Rindt, C.C.M., Zondag, H.A., Zolingen, R.J.Ch., 2010. Detailed analysis of the energy yield of systems with covered sheet-and-tube PVT collectors. Solar Energy, 84, 867-878.

U. S. Department of Energy. Solar Decathlon. 2015. http://energy.gov/, may 2016

Zhang, X., Zhao, X., Xu, J., Yu, X., 2013. Characterization of a solar photovoltaic/loop-heat-pipe heat pump water heating system. Applied Energy, 102, 1229-1245.

Zodang, H.A., De Vries, D.W., Van Helden, W.G.J., Van Zolingen, R.J.C., Van Steenhoven, A.A., 2003. The yield of different combined PV-thermal collector designs. Solar Energy, 74, 253-269.